

Guided Shear Horizontal Surface Acoustic Wave Sensors for Chemical and Biochemical Detection in Liquids

Fabien Josse, Florian Bender, and Richard W. Cernosek

Anal. Chem., **2001**, 73 (24), 5937-5944 • DOI: 10.1021/ac010859e • Publication Date (Web): 15 November 2001

Downloaded from <http://pubs.acs.org> on March 26, 2009

More About This Article

Additional resources and features associated with this article are available within the HTML version:

- Supporting Information
- Links to the 10 articles that cite this article, as of the time of this article download
- Access to high resolution figures
- Links to articles and content related to this article
- Copyright permission to reproduce figures and/or text from this article

[View the Full Text HTML](#)



Guided Shear Horizontal Surface Acoustic Wave Sensors for Chemical and Biochemical Detection in Liquids

Fabien Josse,^{*,†} Florian Bender,[‡] and Richard W. Cernosek^{§,||}

Microsensor Research Laboratory and Department of Electrical and Computer Engineering, Marquette University, P.O. Box 1881, Milwaukee, Wisconsin 53201-1881, Institut für Instrumentelle Analytik, Forschungszentrum Karlsruhe, P.O. Box 3640, 76021 Karlsruhe, Germany, Microsensor Research and Development Department, Sandia National Laboratories, P.O. Box 5800, MS 1425, Albuquerque, New Mexico 87185-1425, and Material Research and Education Center, Department of Mechanical Engineering, 201 Ross Hall, Auburn University, Alabama 36849

The design and performance of guided shear horizontal surface acoustic wave (guided SH-SAW) devices on LiTaO₃ substrates are investigated for high-sensitivity chemical and biochemical sensors in liquids. Despite their structural similarity to Rayleigh SAW, SH-SAWs often propagate slightly deeper within the substrate, hence preventing the implementation of high-sensitivity detectors. The device sensitivity to mass and viscoelastic loading is increased using a thin guiding layer on the device surface. Because of their relatively low shear wave velocity, various polymers including poly(methyl methacrylate) (PMMA) and cyanoethyl cellulose (cured or cross-linked) are investigated as the guiding layers to trap the acoustic energy near the sensing surface. The devices have been tested in biosensing and chemical sensing experiments. Suitable design principles for these applications are discussed with regard to wave guidance, electrical passivation of the interdigital transducers from the liquid environments, acoustic loss, and sensor signal distortion. In biosensing experiments, using near-optimal PMMA thickness of $\sim 2 \mu\text{m}$, mass sensitivity greater than $1500 \text{ Hz}/(\text{ng}/\text{mm}^2)$ is demonstrated, resulting in a minimum detection limit less than $20 \text{ pg}/\text{mm}^2$. For chemical sensor experiments, it is found that optimal waveguide thickness must be modified to account for the chemically sensitive layer which also acts to guide the SH-SAW. A detection limit of 780 ($3 \times$ peak-to-peak noise) or 180 ppb ($3 \times$ rms noise) is estimated from the present measurements for some organic compounds in water.

Acoustic wave-based sensors have been widely investigated and are commonly used for the detection of hazardous compounds in gas environments.¹ More recently, the focus has shifted toward direct liquid-phase sensing applications where the device is in

direct contact with the solution. Here, new challenges are encountered, including additional loss contributions and signal distortions due to the liquid being in contact with the acoustic wave or the interdigital transducers (IDTs). Other challenges include the effects of the liquid seals on signal quality and reproducibility and the transport of the target analyte or antigen to the sensor surface.

Nevertheless, it has been shown that shear acoustic wave devices can be used as sensor platforms in liquid-phase detection.^{2–11} Various types of acoustic waves have been studied, including thickness shear mode (TSM), shear horizontal acoustic plate mode (SH-APM), shear horizontal surface acoustic wave (SH-SAW), and flexural plate wave (FPW). These studies confirm the perturbation of the propagating (or resonating) characteristics of the waves. Of all acoustic wave devices, SH-SAW devices appear most promising for biochemical detection in liquid environments: (1) surface waves are more sensitive than bulk waves to perturbations produced from the environment; (2) the selected piezoelectric materials and transducer designs lead to very high Q (quality factor) structures; (3) device frequencies can be scaled to greater than 100 MHz, so device sensitivity can be high provided that the signal noise can be decreased; and (4) devices are small, robust, and easy to incorporate into on-line low-cost systems. However, despite their structural similarity to Rayleigh

- (2) Andle, J. C.; Vetelino, J. F.; Lade, M. W.; McAllister, D. J. *Sens. Actuators, B* **1992**, *8*, 191–198.
- (3) Andle, J. C.; Weaver, J. T.; McAllister, D. J.; Josse, F.; Vetelino, J. F. *Sens. Actuators, B* **1993**, *13*, 437–442.
- (4) Gizeli, E.; Goddard, N. J.; Stevenson, A. C.; Lowe, C. R. *Sens. Actuators, B* **1992**, *6*, 131–137. Also: *IEEE Trans. Ultrasonics, Ferroelectr. Freq. Control* **1992**, *39*, 657–659.
- (5) Gizeli, E.; Stevenson, A. C.; Goddard, N. J.; Lowe, C. R. *Sens. Actuators, B* **1993**, *13–14*, 638–639.
- (6) Baer, R. L.; Flory, C. A.; Tom-Moy, M.; Solomon, D. S. *IEEE Ultrason. Symp. Proc.* **1992**, 293–298.
- (7) Dahint, R.; Grunze, M.; Josse, F.; Renken, J. *Anal. Chem.* **1994**, *66*, 2888–2892.
- (8) Kondoh, J.; Shiokawa, S. *IEEE Ultrason. Symp. Proc.* **1994**, 507–512.
- (9) Rapp, M.; Wessa, T.; Ache, H. J. *IEEE Ultrason. Symp. Proc.* **1995**, 433–436.
- (10) Welsch, W.; Klein, C.; von Schickfus, M.; Hunklinger, S. *Anal. Chem.* **1996**, *68*, 2000–2004.
- (11) Josse, F.; Zhou, R.; Patel, R.; Zinszer, K.; Cernosek, R. W. *Anal. Chem.* **2000**, *72*, 4888–4898.

[†] Marquette University.

[‡] Forschungszentrum Karlsruhe.

[§] Sandia National Laboratories.

^{||} Auburn University.

(1) Ballantine, D. S.; White, R. M.; Martin, S. J.; Ricco, A. J.; Zellers, E. T.; Frye, G. C.; Wohltjen H. *Acoustic wave sensors: theory, design, and physicochemical applications*; Academic Press Inc.: San Diego, CA, 1997.

SAWs, SH-SAWs often propagate slightly deeper within the substrate (in some cases, referred to as surface skimming bulk waves),^{12,13} hence preventing the implementation of high-sensitivity detectors. The device sensitivity to mass and viscoelastic loadings can be increased using a thin guiding layer on the device surface. The effect of the overlayer is to trap the acoustic energy near the sensing surface,^{12,13} thus increasing the sensitivity to surface perturbations. The resulting acoustic wave is analogous to a Love wave on an isotropic substrate with overlayer.

Various dielectric materials such as silicon dioxide (SiO₂), silicon nitride (Si₃N₄), and most polymers can be used as the waveguide material. Polymers have an advantage over other waveguide materials for Love wave sensor implementation due to their relatively low shear wave velocity⁴ and the ease of surface layer preparation. However, because of their viscoelasticity, cross-linking or curing is necessary to avoid excessive acoustic loss.⁴ Cross-linking allows the acoustically lossy polymer to exhibit an equilibrium elastic stress, thus representing a stable waveguide layer.

However, it is not desirable to simply minimize the acoustic loss of the overlayer. An overlayer with moderate acoustic loss will help to suppress the triple transit echo (TTE), which is one of the major sources of signal distortion for low-loss devices. In addition, for some substrate materials such as 36°YX-LiTaO₃, the overlayer will decrease the acoustic velocity of the SH-SAW, thus reducing signal distortion due to overlap and interference with adjacent bulk waves.

The dielectric overlayer can also act to passivate the IDTs from the contacting liquid, which often is conductive or has a high dielectric constant (like water). Polymers as the passivating coating have a relatively low dielectric constant and will provide an insulating barrier, assuming the polymer is properly cross-linked or cured to eliminate fluid uptake.

Finally, the overlayer has to provide a suitable basis for attachment of selective layers, such as antibodies, enzymes, or chemically selective polymers that will be used to complete the total sensor.

All the above issues must be taken into account when choosing the appropriate waveguide material, determining its thickness and pretreatment (cross-linking process, cure schedule, etc.), and investigating the general design parameters for acoustic wave sensors such as IDT geometry and substrate material.

In the present study, guided SH-SAW devices on LiTaO₃ are investigated for the implementation of high-sensitivity biochemical detectors in liquid environments. Because of their relatively low shear wave velocity, various polymers (cured or cross-linked) are studied as the guiding layer to trap the acoustic energy near the sensing surface. Biosensor and chemical sensor experiments are performed and the results are discussed in terms of sensitivity, detection limit, and reproducibility.

SENSOR DESIGN CONSIDERATIONS

Figure 1 shows the basic configuration of a guided SH-SAW device as a sensor platform. It consists of a SH-SAW device (in this case a delay line) with an overlayer having a lower shear wave velocity. A thin metal layer is used between the two IDTs,

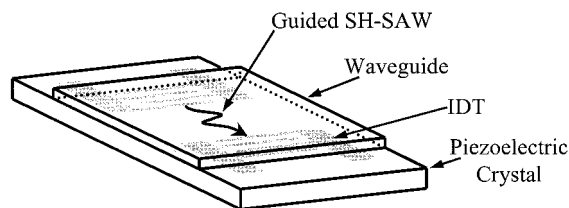


Figure 1. Schematic of a guided SH-SAW device as a sensor platform. For simplicity, only one acoustic delay line is shown.

representing an electrical short and eliminating acoustoelectric interactions with the load. It is the intention of device design to eliminate all electrical load interactions so only sensing caused by mechanical loading is considered here. The effect of the guiding layer is to trap the acoustic energy near the sensing surface, reducing propagation velocity and increasing the sensitivity to surface perturbations.

The first design principles and considerations are identical to those used for Rayleigh SAWs. The design of the IDTs for the generation and detection of SH-SAW uses the delay line configuration often employed for SAW filters. In the present case, a dual delay line design is used with one line as a sensing line and the other as a reference line. Common environmental interactions elicit responses from both lines and are removed by subtraction. The chemical reaction is designed to take place only on the sensing line, and a unique differential signal results. While such a design is usually made with few engineering considerations, analysis or prediction of the sensor response requires that the sensor effect be accounted for in the device response. The sensor effect can be easily incorporated into the device unperturbed transfer function, $T_{12}(f)$, to allow for the variations of delay time and attenuation. The sensor response can then be modeled by the following transfer function

$$T_2(f) = T_{12}(f) e^{-i(2\pi l/\lambda)} e^{i(2\pi\delta l_s/\lambda)} e^{-\alpha l_s} \quad (1)$$

where $\delta \equiv \Delta V/V$ is the fractional velocity change of the SH-SAW due to the sensing effect, λ is wavelength, α is the attenuation coefficient introduced by the waveguide layer and chemically sensitive layer composite, and l and l_s are the IDT center-to-center separation and sensing path length, respectively.

In the case of a guided SH-SAW, waveguiding by a suitable layer (oxide coating, polymer, polyimide, etc.) of appropriate thickness occurs when the shear wave velocity in the layer (V_M) is less than that in the substrate (V_{SH}). Assuming that a predominantly shear horizontal wave is coupled to the IDT, the fractional change in the wave velocity, a measure of the sensitivity to surface mechanical perturbations, can be obtained from perturbation theory¹⁴ as

$$\frac{\Delta V}{V} = -\frac{V_{SH}}{4}(\rho h) \left[1 - \left(\frac{V_M}{V_{SH}} \right)^2 \right] |U_2|^2 \quad (2)$$

where V_{SH} is the unperturbed velocity of the SH-SAW, ρ is the layer mass density, h is the layer thickness, and U_2 is the

(12) Lee, D. L. *IEEE Trans. Son. Ultrason.* **1981**, *28*, 330–341.

(13) Josse, F.; Lee, D. L. *IEEE Trans. Son. Ultrason.* **1982**, *SU-29* (No. 5), 262–273.

(14) Auld, B. A. *Acoustic Fields and Waves in Solids*, 2nd ed.; Krieger: Malabar, FL, 1990; Vol. II.

normalized particle velocity displacement amplitude at the surface; ρh represents the mass load per unit surface area. It is noted that when the resulting wave suffers no dispersion, and the sensing path length, l_s , is equal to the propagation path length, l , eq 2 also describes the relative frequency shift, $\Delta f/f$, of the guided SH-SAW sensor. As a result, the device sensitivity to mass and viscoelastic loadings due to the thin guiding layer can be calculated.^{15–18} Writing $\Delta m = \rho h$, the device sensitivity to mass loading can be defined in terms of $\Delta V/V$ or $\Delta f/f$ as

$$S_m = \lim_{\Delta m \rightarrow 0} \left(\frac{\Delta f}{f} \right) / \Delta m \quad (3)$$

The above assumes a purely elastic, lossless film. It is also noted that for a lossless film the term $e^{-\alpha l}$ in eq 1 is equal to 1. Clearly, the device sensitivity increases as U_2 at the sensing surface increases, i.e., as the acoustic energy is trapped to the sensing surface. However, for viscoelastic film loading, the device sensitivity to mass loading or viscoelastic loading should be calculated. In that case, the waveguiding layer and the biochemically sensitive layer are characterized by a complex shear modulus, $\mu' + j\mu''$, with $\mu'' = \omega\eta$. μ' and μ'' are the shear storage modulus and loss modulus, respectively, η is the shear viscosity coefficient, and $\omega = 2\pi f$ is the angular frequency. While mass loading is often assumed the dominant factor contributing to the frequency change, viscoelastic properties also contribute to Δf changes and lead to changes in device attenuation. In the latter case, changes in the device loss can be used as a second measurand to characterize the sensor. For low-loss surface materials, and assuming $h \ll \lambda$, approximate analytical expressions can be obtained for both the velocity change and the attenuation.¹ For the 36°YX-LiTaO₃, such an expression for the attenuation coefficient must also account for the effect of the shear vertical (SV) wave component, which is not negligible in evaluating the loss. In that case, eq 2 can still be used to approximate the velocity change. However, for arbitrary viscoelastic film loading, effective computation of both parameters can only be achieved numerically. This decision is made depending on the value of the mechanical quality factor, Q , of the load. It is noted the inverse of Q is defined as the loss tangent, $\tan \theta \equiv 1/Q = \mu''/\mu'$, and if $\tan \theta > 0.1$, then the load material may be treated as a lossy medium.¹⁹

For biosensing applications in which a second layer (the layer of attached receptors) is applied on the waveguide layer, eq 3 is sufficient to approximate the mass sensitivity of the device.^{15,18} This is because the bilayer consisting of the receptors and the bound antigens is of the order of a few molecules and has negligible viscoelastic contribution to the sensor response. For chemical sensors in which a chemically sensitive and lossy polymer is deposited on the guiding layer, the value of the mechanical quality factor, Q , will dictate the approach to use in evaluating the device attenuation in terms of the layer thickness and viscosity.

EXPERIMENTS

Devices. The piezoelectric substrate material used for the guided SH-SAW devices is 36°YX-LiTaO₃. Devices are fabricated with 90-nm-thick Cr/Au (20/70 nm) split finger IDTs having a period of 40 μm , which corresponds to an operating frequency of ~ 103 MHz for the uncoated device. A dual delay line configuration is used with a metallized delay path (a thin Cr/Au (20/70 nm)) to eliminate acoustoelectric interaction with the load. The delay time of the device is ~ 2.15 μs . Using a dual delay line configuration with one line as the reference line and the other as the sensing line makes temperature control essentially unnecessary. Temperature fluctuations and other nonspecific detections are canceled out. Poly(methyl methacrylate) (PMMA) and cyanoethylcellulose (CEC) were selected as the coating materials. The PMMA and CEC waveguide layers were deposited on the device surface (over the IDTs and the delay path) by spin-coating solutions of 10 and 20% w/v PMMA (35 000 g/mol) in 2-ethoxyethyl acetate and CEC/tetraglycidyl diaminediphenylmethane (the cross-linking agent) in dimethylformamide. The polymer layers were then cured by heating at 180 °C for 2 h. Depending on solution concentration and spin speed, waveguide thicknesses in the ranges 0–3.2 and 0–4 μm have been obtained, as determined by profilometry. It is noted that other challenges exist that affect device performance. These include possible fluctuations in electrical properties and viscosity of the analyte solution as well as the need to press a liquid seal onto the device surface. These perturbations can affect loss and signal stability of the device, offset sensitivity, or create a lack of reproducibility of experimental results. The delay path metallization and the guiding layer (if thickness is properly selected) will eliminate acoustoelectric interactions with the latter providing sufficient electrical passivation of the IDTs.

Test Hardware, Experimental Setup, and Procedures. A special flow-through cell was designed to expose each guided SH-SAW dual delay line device to the biological or chemical environments and to interrogate them electrically. For initial device characterization, a network analyzer (HP 8751A) was used. A signal generator (HP 8656B) and a vector voltmeter (HP 8508A) were used for the sensing experiments, together with a switch/control unit (HP 3488A) and a multimeter (HP 3457A). The experimental setup was composed of the sensing system, the sample delivery system, and the electronic instrumentation as described in ref 20. The sensing system consisted of the guided SH-SAW devices, the mounting elements, and a measurement cell made from brass and Lexan. In the solvent detection experiments, the liquid delivery system consists of a sample tank, a flow injection analysis system (Alitea FIALab-3500), and a working solution. For some of the experiments, a second flow injection analyzer (Eppendorf) was used. Well-defined concentrations of organic analytes were prepared by diluting the organic compounds in deionized (DI) water and injected into the working solution by the computer-controlled flow injection analysis system. A typical run was started by pumping DI water through the cell at a selected flow rate. A low flow rate of 0.30 mL/min was used to minimize the hydrodynamic coupling between flowing liquid and crystal surface, the pressure and pulsating flow effects (for the Eppendorf flow injection analyzer) on the sensor surface that can add to the device noise. Stability of the frequency response is first established

(15) Andle, J. C.; Vetelino, J. F.; Josse, F. *IEEE Ultrason. Symp. Proc.* **1991**, 285–288.

(16) Kovacs, G.; Venema, A. *Appl. Phys. Lett.* **1992**, *61*, 639–641.

(17) Wang, Z.; Cheeke, J. D. N.; Jen, C. K. *Appl. Phys. Lett.* **1994**, *64*, 2940–2942.

(18) Du, J.; Harding, G. L. *Sens. Actuators, A* **1998**, *65*, 152–159.

(19) Kielczynski, P. *J. Appl. Phys.* **1997**, *82*, 5932–5937.

(20) Bender, F.; Cernosek, R. W.; Josse, F. *Electron. Lett.* **2000**, *36*, 1672–1673.

for ~20 min. This DI water baseline was then followed by a series of exposures to the analyte solutions.

When both the sensing and reference lines were used, temperature control was essentially unnecessary. Only the solvent samples were placed in a common water bath to stabilize their temperature with the ambient.

Reagents. The liquids were prepared from analytical-grade reagents, purchased from Aldrich (Milwaukee, WI), and used as received. The polymers were also purchased from Aldrich. For all testing, DI water was used.

Biochemical Preparation. The sensor surfaces were cleaned for 30 min in 0.1 M HCl in DI water/ethanol (1/1). Next, one delay line (sensing line) was exposed to a solution of 7 μg of goat immunoglobulin G (IgG) in 0.7 mL of phosphate-buffered saline (PBS) for 60 min. Finally, both delay lines were exposed to a solution of 10 mg of bovine serum albumin (BSA) in 1 mL of tris-(hydroxymethyl)aminomethane buffer for 60 min in order to saturate binding sites for protein adsorption. Each step was followed with rinsing in PBS.

Preparation for Solvent Detection. On some of the devices (PMMA waveguide thicknesses 0–1.8 μm), the sensing line was covered with an additional polymer film to provide partial chemical selectivity. Films of poly(isobutylene) (PIB), poly(vinyl acetate) (PVAC), poly(vinylbutyral) (PVB), poly(ethyl acrylate) (PEA) and poly(diphenoxyphosphazene) (PDPP) were deposited. All the films were spin-coated and cured for 5–10 min at temperatures of 40–45 $^{\circ}\text{C}$. The lower temperature cure reduces film stiffening and allows for maximum solvent uptake. The tested organic analytes are tetrachloroethane, tetrachloroethylene, trichloroethylene, tetrachloromethane, chloroform, toluene, (*m*-, *o*-, *p*-)xylenes, cyclohexane, hexane, benzene, and ethylbenzene.

RESULTS AND DISCUSSION

In liquid-phase applications, stability of the sensor platform is essential for reusability and repeatability. Because these sensor properties can be affected by the waveguide layer stability in water, it was important to cure (or cross-link) the guide polymer. Figure 2 shows the effect of the polymer curing on device loss over a 3-h period at 180 $^{\circ}\text{C}$. The changes (decreases) in device loss clearly indicate the coating becomes more elastic (glassy), thus decreasing water uptake and improving stability. Also, temperature curing has basically the same effect on the coating viscoelasticity as cross-linking. Moreover, curing for 2 h was indeed sufficient to achieve a stable polymer. Finally, it is noted that the cured film was continuously subjected to water for over 1 week with little degradation of the device response.

Figure 3 shows the frequency shift (sensitivity) of the LiTaO₃ guided SH-SAW as a function of the PMMA and CEC layer thickness. It can be seen that the slope of the curve in Figure 3 reaches a maximum at a waveguide thickness of between 1600 and 2000 nm for the PMMA, indicating the near-optimum thickness for achieving high mass sensitivity. For CEC, an optimum thickness of ~2400 nm was determined. An effective determination of the optimum thickness, however, requires looking at the device insertion loss in liquid environments as well as the frequency shift.

An advantage of the guiding layer (if appropriately selected) is the protection—specifically passivation of the IDTs. The piezoelectric substrate materials most commonly used for guided

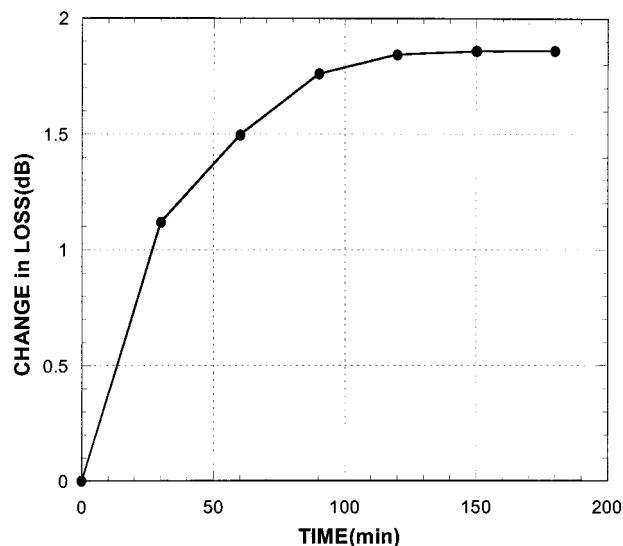


Figure 2. Changes in guided SH-SAW device loss versus curing time for a 2- μm -thick PMMA coating on 36 $^{\circ}$ YX-LiTaO₃, indicating effect of viscoelasticity change. Curing temperature is 180 $^{\circ}\text{C}$.

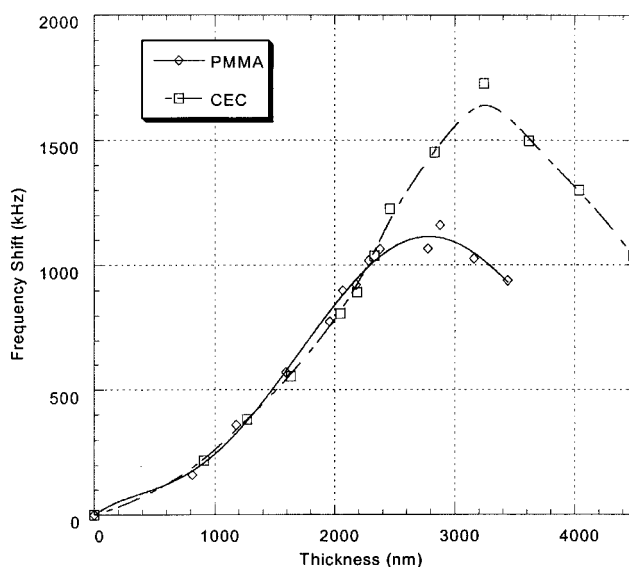


Figure 3. Guided SH-SAW frequency shifts (or sensitivity) for PMMA and CEC guiding layers as a function of layer thickness.

SH-SAW sensors are quartz and LiTaO₃. The latter has the advantages of both a high piezoelectric coupling constant and a high dielectric constant of $\epsilon = 47$.^{7,8} The high piezoelectric coupling constant allows the implementation of low-loss acoustic devices, and the high dielectric constant helps confine a sufficient portion of the electric fields generated by the IDTs to the substrate, even in direct contact with aqueous solutions ($\epsilon = 75$). In the case of quartz, the low dielectric constant of $\epsilon = 4.5$ –4.7 makes it difficult to confine a significant portion of the electric fields to the substrate in the presence of the aqueous solutions. This necessitates the use of either thick coatings over the IDTs^{18,21} or a flow cell confining the liquid to the area between the IDTs. However, liquid seals on the sensing surface (between the IDTs) could introduce a distortion of the wave front, hence sensor signal degradation.

(21) Leidl, A.; Filser, H.; Labatzki, A. *Sens. Actuators, A* **1995**, *47*, 353–356.

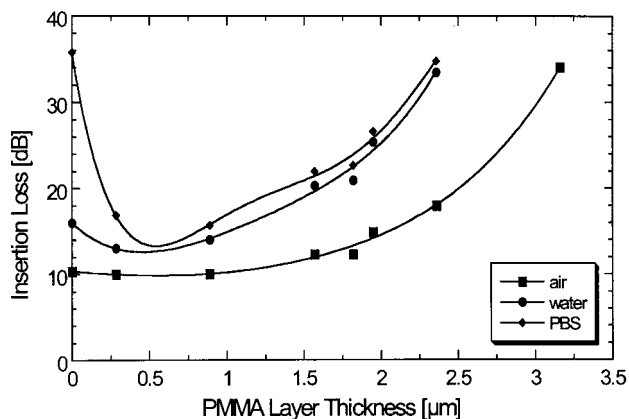


Figure 4. Insertion loss as a function of PMMA waveguide thickness for the guided SH-SAW sensors operated in the indicated media.

For the LiTaO_3 devices, immersing the IDTs in liquid does not cause significant problems. Several devices with waveguide thicknesses ranging from 0 to $3.2 \mu\text{m}$ have been characterized.²⁰ The insertion loss as a function of waveguide thickness is shown in Figure 4 for three different boundary conditions (the entire coated surface exposed to air, DI water, and PBS, respectively). It is seen that the loss in air increases sharply with increasing PMMA thickness of $\sim 2.0 \mu\text{m}$. This is due to overconfinement of the wave to the surface layer, resulting in both an increased acoustic loss due to the polymer and a decrease in coupling efficiency of the IDTs. In water, the increase in the insertion loss is even more abrupt starting at $\sim 1.0 \mu\text{m}$. At a PMMA thickness of $\sim 2.5 \mu\text{m}$, the acoustic attenuation becomes too large for proper sensor operation. At this thickness, overconfinement of the wave to the surface increases the acoustic coupling to the liquid medium. The PMMA also absorbs a small amount of water, which compounds the increased insertion loss at greater thicknesses.

On the other hand, a very thin polymer layer (less than $1.0 \mu\text{m}$) effectively isolates the IDTs electrically from the liquid. This can be seen when the curves for water and PBS are compared in Figure 4. Such a thin polymer layer, however, does not efficiently trap the acoustic energy near the sensing surface and optimize detection sensitivity. It is found that if the PMMA guiding layer is too thick ($\gg 2 \mu\text{m}$), the acoustic attenuation becomes too high. Thus, a compromise in waveguide thickness must be made, combining a high sensitivity with a moderate loss. Such a tradeoff between high sensitivity and low loss results in an optimum PMMA thickness of $\sim 2.0\text{--}2.3 \mu\text{m}$. This thickness is not too different from that determined from measuring the frequency shift in air (Figure 3).

Biosensors and Effect of PMMA Layer Thickness on Mass Sensitivity. In this section and the following section on Chemical Sensors, only the results from devices using the PMMA guiding layers will be shown and discussed. To evaluate the mass sensitivity of the guided SH-SAW device, biosensing experiments were conducted with goat IgG adsorbed on one delay line of the dual delay line device while the other delay line was blocked with BSA. The device was then exposed to rabbit anti-goat IgG in the liquid environment. In Figure 5, the responses of devices with different PMMA coating thicknesses to injection of $24 \mu\text{g/mL}$ rabbit anti-goat IgG are shown. The difference signal (sensing line minus reference line) is plotted. It is obvious that mass

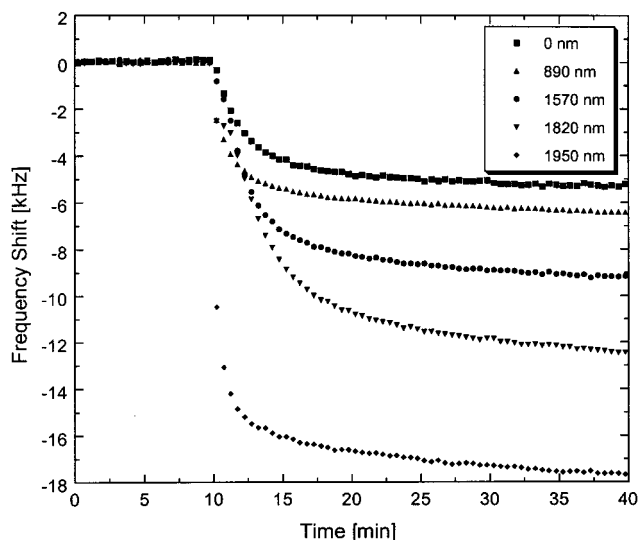


Figure 5. Responses of guided SH-SAW devices with PMMA coatings of the indicated thicknesses to injection of $24 \mu\text{g/mL}$ rabbit anti-goat IgG. The difference signal (sensing minus reference lines) is shown.

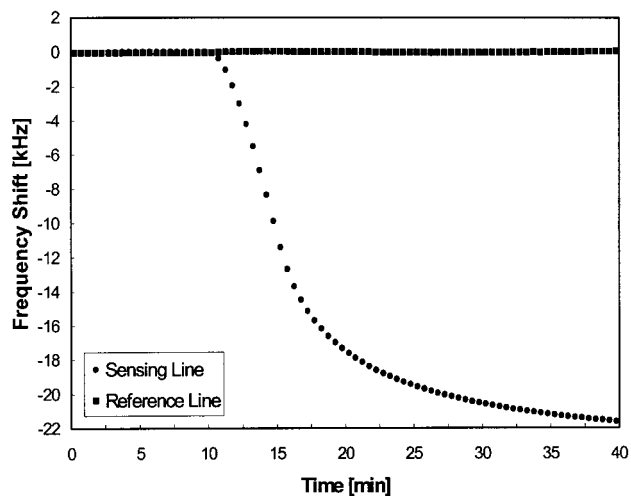


Figure 6. Frequency responses of the two delay lines of a guided SH-SAW device to $3 \mu\text{g/mL}$ rabbit anti-goat IgG, injected after 10 min. The device has a PMMA waveguide of $2.2\text{-}\mu\text{m}$ thickness.

sensitivity increases with waveguide thickness, while differences in baseline noise are small. Clearly, as the film thickness increases, the acoustic energy is trapped more to the sensing surface, drastically increasing the device sensitivity. The frequency shift produced in a sensor with 1950 nm of PMMA is more than 4 times greater than that for a sensor with no PMMA waveguide. Figure 6 shows the detection of $3 \mu\text{g/mL}$ rabbit anti-goat IgG by a device coated with $2.2\text{-}\mu\text{m}$ PMMA (and goat IgG on the sensing line). The frequency responses of the two delay lines are plotted separately. As the figure shows, the entire frequency shift of over 20 kHz is due to antibody–antigen binding; the reference line (which is also exposed to the injected antibody) does not respond significantly. The responses are not corrected for the influence of temperature, and no effort was made to control laboratory or device temperature.

To compare the mass sensitivities of the guided SH-SAW devices, two TSM resonators were treated in the same manner as the sensing lines of the guided SH-SAW sensors, and the same

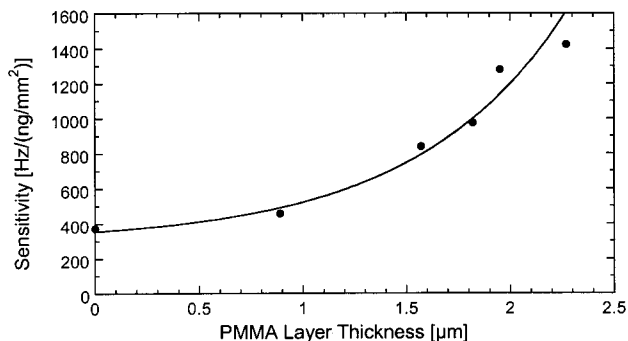


Figure 7. Mass sensitivities of guided SH-SAW devices with PMMA coating thicknesses of 0–2.27 μm , calibrated using two TSM resonators.

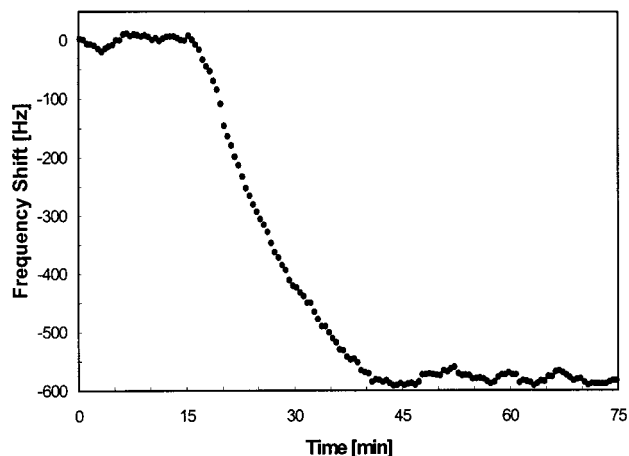


Figure 8. Response of a guided SH-SAW device with 1.57- μm -thick PMMA coating to 100 ng/mL rabbit anti-goat IgG, injected after 15 min. The difference signal (sensing minus reference lines) is shown.

biochemical experiments were performed. Using the Sauerbrey equation,²² these experiments revealed a mass density of the deposited rabbit anti-goat IgG layer of 17 ng/mm², corresponding to a closely packed monolayer of antibodies on the resonator active surface area. This value was then used to calibrate the guided SH-SAW sensors. Figure 7 shows the results for guided SH-SAW devices with PMMA coating thicknesses of 0–2.27 μm . Mass sensitivities up to 1420 Hz/(ng/mm²) have been obtained. This value must be compared to the baseline noise level in order to estimate the minimum detection limit of the devices. Note the detection limit can be defined as either 3 times the peak-to-peak noise or 3 times the root-mean-square (rms) noise; both definitions have been used in the literature.

Because the phase was measured using a signal generator and a vector voltmeter, the experiments were designed to obtain a maximum amount of information rather than to minimize the noise. However, in an attempt to further reduce the noise, the data collection software was modified for the detection of small antibody concentrations by averaging the data taken over a period of 5 min. Figure 8 shows the detection of 100 ng/mL rabbit anti-goat IgG by a 1.57- μm -thick waveguide device (note this PMMA layer thickness is nonoptimal). Noise levels of 32 (peak to peak) and 8 Hz (rms) were obtained. These results reveal the most

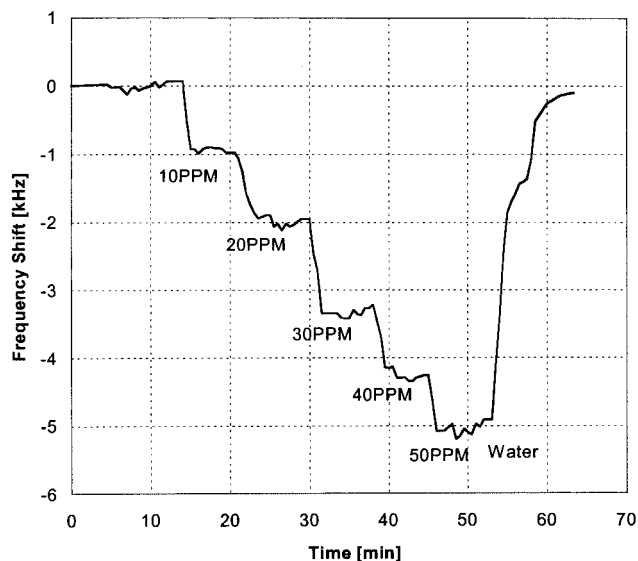


Figure 9. Detection of 10–50 ppm PCE in DI water using a guided SH-SAW device with 0.8- μm PEA layer deposited on 0.3- μm -thick PMMA waveguide layer. No reference line was used in these measurements.

sensitive device can detect 68 or 17 pg/mm², respectively, the latter corresponding to 0.1% of a closely packed monolayer of antibodies.

It was found that cleaning the device with a swab stick soaked in ethanol allowed the biosensor surfaces to be reclaimed and then used a number of times without removing the PMMA layer. Excellent reproducibility in the mass sensitivity of the devices was observed. However, if the PMMA layer is damaged over time and the device becomes too lossy, it is also possible to remove the coating completely by immersing the device in concentrated acetone for a few hours. A new PMMA layer can then readily be deposited. No aging could be observed in the other components of the SH-SAW devices over a period of more than 1 year.

Chemical Sensors. To demonstrate the versatility of the guided SH-SAW sensor concept, the devices were also tested in detection of trace chemical contaminants in aqueous environments. The chemically selective polymer layers were deposited as a second layer on the PMMA. Since the devices with moderate PMMA waveguide thicknesses (0.5–1.5 μm) can be operated in a liquid environment with insertion losses of only 13–16 dB (see Figure 3), even soft and porous polymer layers can still be added without exceeding the limits of tolerable overall loss. This allows one to combine high solvent uptake of the chemically sensitive polymer with low signal noise. Different thickness combinations of PMMA waveguide and chemically sensitive layers are tested. It is noted that, because of the difference in viscoelasticity between the two layers, the results in Figures 3 and 4 can only serve as a guide to define the thickness combination for optimum sensitivity. In what follows, only results for selected organic solvent detection will be shown and discussed.

Figure 9 shows the response of a guided SH-SAW sensor device to various concentrations of tetrachloroethylene (PCE) in DI water. On that device, the chemically sensitive polymer is a 0.8- μm -thick PEA layer spin-coated on a 0.3- μm -thick PMMA waveguide. The results demonstrate a direct detection of 10 ppm PCE in water as well as excellent reversibility when the chemical

(22) Sauerbrey, G. *Z. Phys.* **1959**, *155*, 206–212 (in German).

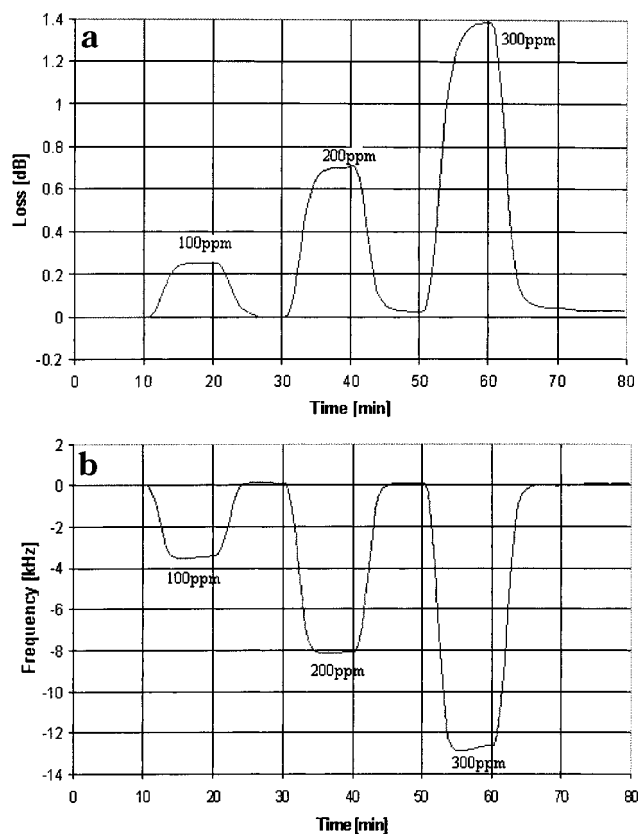


Figure 10. Detection of 100–300 ppm toluene in DI water using a guided SH-SAW device with 0.4- μm PIB layer on 0.3- μm PMMA waveguide. After each concentration step, DI water was delivered to the device for 10 min to see if the signal would return to baseline. The difference signals are shown: (a) change in device insertion loss; (b) frequency shifts.

is removed. However, Figure 9 also shows that significant noise exists; reducing these noise levels will require utilization of the reference line to minimize all secondary effects.

Figure 10 shows the detection of toluene in DI water at concentrations of 100–300 ppm. The sensing line of the device was covered with a 0.3- μm -thick PMMA waveguide layer and an additional layer of $\sim 0.4\text{-}\mu\text{m}$ -thick PIB, the latter being a good sorbent medium for toluene and a poor sorber of water. The reference line was covered with $\sim 0.9\text{-}\mu\text{m}$ PMMA. A good signal-to-noise ratio is observed, as well as rapid response and recovery times (<2 min.). The observed frequency shift (Figure 10b) is reversible and approximately linear with analyte concentration. Figure 10a shows the measured change in device loss, which can also be used as a second sensor parameter. This parameter may prove useful in the analysis of sensor array responses when analyte specificity is extracted. It is noted that the loss data are not linear with toluene concentration (within the measured range) and thus indicate a level of independence from the frequency shift data in Figure 10b. The measured loss nonlinearity may be attributed to a change in the viscoelastic properties of the chemically sensitive coating, which plasticizes upon absorption of the solvent. In Figure 11, the results for the detection of ethylbenzene are shown using the same device utilized for the results shown in Figure 10. In the experiments leading to Figure 11, an attempt was made to demonstrate repeatability for the detection of 100 ppm ethylbenzene using 10-min analyte exposures followed by 10-min DI water

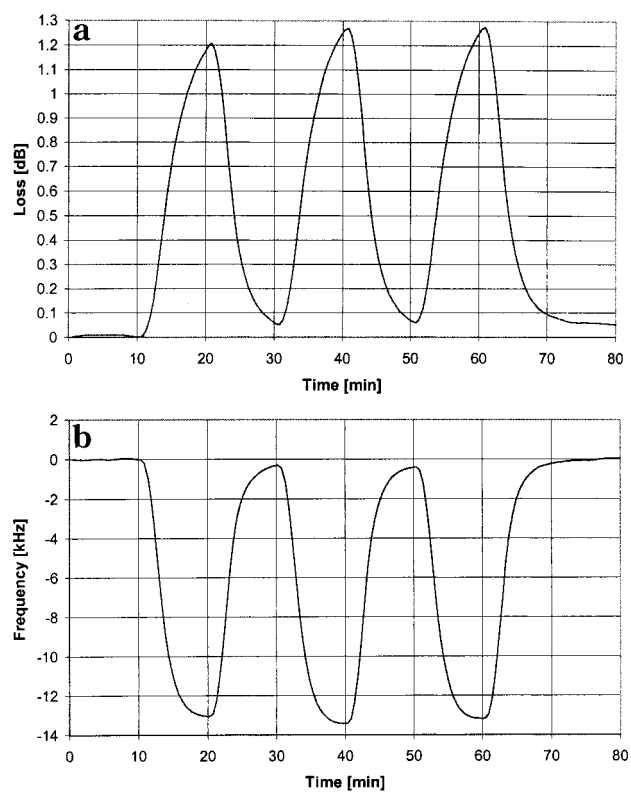


Figure 11. Repeated detection of 100 ppm ethylbenzene in DI water a guided SH-SAW device with a PIB layer. The device was then exposed to DI water for reusability. This process was repeated several times.

Table 1. Sensitivities (in Hz/ppm) of Three Different Guided SH-SAW Devices to Three Different Solvents^a

| solvent | no waveguide | 0.3- μm PMMA | 1.8- μm PMMA |
|---------------------|--------------|-------------------------|-------------------------|
| toluene | -46 | -41 | -21.5 |
| trichloroethane | -16 | -16.3 | -10.6 |
| tetrachloroethylene | -130 | -124 | -116 |

^a In each case, the sensing line was covered with $\sim 0.4\text{-}\mu\text{m}$ PIB, deposited on top of the indicated waveguide. The reference lines were covered with 0.6-, 0.9-, and 1.8- μm PMMA, respectively.

exposures. Device response repeatability is good although PIB desorption of the ethylbenzene takes longer than the 10-min period when the analyte is not present.

To quantify the influence of waveguide thickness on sensitivity and baseline stability, devices with different PMMA thicknesses have been compared in solvent detection experiments. Preliminary results are given in Table 1 for the PIB-coated devices. All PIB layers were 0.4 μm and deposited only on the sensing line over the PMMA layer. PMMA waveguide layer thicknesses were 0.6 μm on the reference line and 0 μm on the sensing line of the first device, 0.9 μm on the reference line and 0.3 μm on the sensing line of the second device (same device used to produce results shown in Figures 10 and 11), and 1.8 μm on both lines of the third device. The data in Table 1 show that, for PCE, a sensitivity of 130 Hz/ppm was achieved using only the PIB film on the sensing line. Given the noise values determined previously, this corresponds to a minimum detection limit of 740 or 185 ppb PCE, respectively. Adding a thin PMMA waveguide layer (0.3 μm)

results in similar sensitivities for all three solvents. The use of a thick guiding film (1.8 μm) shows a decrease in sensitivity. The latter result is in conflict with the results from the biosensing experiments, but it can be better understood if the viscoelastic contributions to the sensor response are taken into account. In the biosensing experiments, only an acoustically thin layer was deposited on top of the PMMA coating during antibody–antigen binding. Thus, the device mainly responds to the mass loading. However, in the case of solvent detection, the PIB layer on top of the waveguide will absorb the solvent, resulting in changes in elastic constants and acoustic dissipation in the polymer film. Thus, the device can no longer be considered a pure mass detector. This is also confirmed by an increase in loss during solvent uptake of over 2 dB in some cases. Also, it is noted that PIB absorbs very little water while exhibiting a high affinity for the low concentrations of solvents tested. This means the PIB is acting mostly as a waveguide, and it appears that the 0.4- μm PIB layer alone (no PMMA) might be a near-optimal thickness for this sensor configuration. It should be pointed out that the observed absolute values for the loss before analyte exposure were quite high for the PMMA plus PIB films. For example, for the 1.8- μm PMMA plus 0.4- μm PIB film, the starting value for the loss was ~ 30 dB. The relative changes in loss are less than 1.7×10^{-2} dB/ppm for analyte exposure. It is possible that the large attenuation due to the thick composite layer (PMMA/PIB) reduces the device sensitivity. More work is under way to determine the trend in sensitivity with the composite layer thickness and the effect of the overall (waveguide layer plus chemically sorbent coating) viscoelasticity on the sensitivity response. No effect of film resonance on the device sensitivity has been observed for the film thicknesses investigated in the present work.

It is noted that the above chemical sensor results are far from being optimized. Arbitrary nonoptimum combinations of guiding layer and sensing layer thicknesses were chosen for testing. The selected chemically sorbent coatings are taken from our existing film library generated for similar work in liquid environments using TSM resonators¹¹ and from the published literature in gas sensing.¹ Many coating materials are available. In addition to the desired characteristics discussed previously, the only other requirement for polymer sensing layer selection is stability in water. Several other sensor coating polymers that could act as both the guiding layer and the chemically sensitive layer, as well as molecularly imprinted polymers (templating), need to be investigated to take advantage of the high sensitivity offered by the guided SH-SAW in liquid chemical sensing applications.

CONCLUSIONS

It was demonstrated that the guided SH-SAW on 36°YX-LiTaO₃ substrates can be used for high-sensitivity sensor implementation in liquid environments. In biosensing experiments, mass sensitivities as large as 1420 Hz/(ng/mm²) have been achieved. It must be noted that the devices used were yet to be optimized for maximum sensitivity. To achieve a higher sensitivity one must select a waveguiding polymer material for a given application and then determine its optimum thickness. Devices operating at 103 MHz were used in the current studies, but increasing the operating frequency will also help increase the resolution of the sensor while requiring a thinner layer for optimal waveguiding.

In addition, by using unidirectional IDTs or an efficient IDT resonator design, the total loss of the devices can be reduced, allowing for greater attenuation in the waveguide layer if optimization requires thicker films. While a resonator configuration may be more sensitive in some cases (low loss, hence high Q) than the delay line configuration, modeling and predicting the sensor response accounting for the added analyte perturbations becomes more difficult. In that case, detection mechanisms include mechanical loading (mass and viscoelasticity), electrical loading (dielectric and conductivity effects), and some transduction effects within the IDT region.

A particular advantage of the LiTaO₃ device substrate used for these experiments is that the liquid needs not be confined to the area between the IDTs. Therefore, seals are not needed in the acoustic wave propagation path where detection occurs. This reduces signal loss and distortion and ensures reproducibility and stability of the experiments. In addition, the low acoustic loss observed for thin PMMA and CEC waveguides allows for adding lossy sensing layers, which makes the device suitable for a number of liquid chemical applications.

It was found that easy-to-prepare polymers represent effective waveguides. Sufficient chemical and mechanical robustness has been obtained for cured PMMA films that behave acoustically like a cross-linked PMMA with improved stability in water. For the LiTaO₃ substrate, electrical passivation of the IDTs can easily be achieved with thin polymer films ($< 1 \mu\text{m}$). Issues still to be addressed are the acoustic loss of the PMMA and its tendency to absorb a small amount of water after repeated use (over 1 week). The CEC and other polymer materials (polyimides and other photoresists) need to be investigated for applications in which PMMA is not suitable.

The biosensing experiments revealed an optimum PMMA waveguide thickness of 2.0–2.3 μm . However, in the solvent detection experiments, a comparable waveguide thickness did not prove useful. This discrepancy was attributed to the fact that sensors with thick waveguides and additional lossy polymers on top of the waveguides no longer behave as classic mass detectors. Instead, the viscoelastic behavior of the polymer films must be taken into account to find the optimum thickness combinations of the sensing layer and the guiding layer.

ACKNOWLEDGMENT

The authors gratefully acknowledge Dr. Antonio J. Ricco of ACLARA Biosciences and Dr. Rongnong Zhou of Marquette University for valuable assistance and helpful discussions, and Kristofer Zinszer of Marquette University for performing some of the experiments. The authors also thank W. G. Yelton, M.A. Mitchell, A. N. Rumpf, and A. W. Staton for helpful technical assistance. This project was funded in part by the National Science Foundation (NSF), and the U.S. Department of Energy, Office of Nonproliferation and National Security. Sandia is a multiprogram laboratory operated by Sandia Corp., a Lockheed Martin Co., for the United States Department of Energy under Contract DE-AC04-94AL85000.

Received for review July 31, 2001. Accepted October 9, 2001.

AC010859E